Imprints of accretion on gravitational waves from black holes

Philippos Papadopoulos[1] and José A. Font[2]

(1) School of Computer Science and Mathematics, University of Portsmouth, PO1 2EG, Portsmouth, United Kingdom

(2) Max-Planck-Institut für Astrophysik, Karl-Schwarzschild-Str. 1, D-85740 Garching, Germany

(October 27, 2018)

Abstract

Black holes are superb sources of gravitational wave signals, for example when they are born in stellar collapse. We explore the subtleties that may emerge if mass accretion events increase significantly the mass of the black hole during its gravitational wave emission. We find the familiar damped-oscillatory radiative decay but now both decay rate and frequencies are *modulated* by the mass accretion rate. Any appreciable increase in the horizon mass during emission reflects on the instantaneous signal frequency, which shows a prominent negative branch in the $\dot{f}(f)$ evolution diagram. The features of the frequency evolution pattern reveal key properties of the accretion event, such as the total accreted mass and the accretion rate. For slow accretion rates the frequency evolution follows verbatim the accretion rate, as expected from dimensional arguments. In view of the possibility of detection of black hole "ringing" by the upcoming gravitational wave experiments, the deciphering of the late time frequency dynamics may provide direct insight into otherwise obscured aspects of the black hole birth process.

PACS numbers: 04.25.Dm, 04.40.-b, 04.70.Bw, 95.30.Lz

The classic black hole solutions of the Einstein equations are an enduring achievement of general relativistic theory research as evidenced by the increasing attention they receive in observational programmes in astrophysics and gravitational wave (GRW) science. *Linearised perturbation* studies of such spacetimes are by now fairly thoroughly understood (see [1,2]) and conclude that the governing dynamical equations for perturbations of any spin (scalar, electromagnetic and gravitational) are all mapped into wave equations with a short range potential. Among the solutions of those equations pre-eminent role is reserved for the damped oscillating modes (out-going at infinity and in-going at the horizon), the so-called quasi-normal modes (QNM). Physically, and in the language of GRW signals, a generic excitation of an isolated black hole leads to a prompt emission, followed by the exponentially decaying QNM ringing. The latter is quickly dominated by the slowest damped mode. A review of this phenomenology is given in [3]. An extension of the vacuum black hole paradigm is given in [10]. This study concerned the computation of QNM frequencies in the presence of matter shells, but is limited to ad-hoc static spherical configurations. Another class of simple spherically symmetric solutions, those describing collapse of compact lumps of matter, has also received wide attention [4,5]. Extensively used in conjunction with perturbation theory [6,7], those solutions helped elucidate the GRW signals expected from stellar collapse. These studies showed that the end-stages of the emission during gravitational collapse may be dominated by the QNM ringing of the emerging black hole, in particular the *single* QNM frequency of the least damped mode. Early numerical relativity studies seem to corroborate this picture [8].

The precise dynamics of stellar collapse remains controversial, especially for more massive stars. A range of so called "collapsar" models (see e.g., [9] and references therein) speculate that significant amounts of matter will accrete immediately *after* the black hole has formed, possibly at very high accretion rates. An expanding while radiating black hole is possible even in complete absence of matter, e.g., in the coalescence of a binary black hole. The paradigms of stationary vacuum black hole and simple spherical collapse perturbations are perhaps inadequate models for GRW emission in such cases, but the literature appears not

to have addressed the issue at all. In this work we initiate a study of this regime using numerical, fully relativistic, solutions of accreting black hole spacetimes and we model non-spherical spacetime perturbations using the dynamics of a scalar field on this time-dependent background. We find that accretion extends the phenomenology of black hole ring-down in a well defined manner. The resulting GRW signals are best described as amplitude and frequency (AM/FM) modulated versions of the simple damped sinusoidal waveforms.

The first major component of the investigation is the self-consistent relativistic description of a growing, spherically symmetric, black hole spacetime. To our knowledge there exists no simple model for such spacetimes, hence we resort to numerical simulation. As a sufficient, not unduly specialised, model of an accreting black hole we solve the coupled system of Einstein's field equations and perfect fluid hydrodynamics in spherical symmetry as in [11]. The spacetime geometry is described in the Tamburino - Winicour framework [12], which provides a *characteristic initial value formulation* for the system of Einstein's equations. The computational domain is bounded by a worldtube W. The metric element is explicitly $ds^2 = -e^{2\beta}V/rd\tau^2 + 2e^{2\beta}d\tau dr + r^2 d\Omega^2$, in geometrised units ($G = c = 1$). The geometry is described by the two metric functions $\beta(\tau, r)$ and $V(\tau, r)$. They obey radial hypersurface equations, with the stress-energy tensor of the fluid acting as a source term. Our setup uses lightcones converging to the interior of W and intersecting the black hole horizon. In the case of a static *vacuum* black hole, this would correspond to advanced time (ingoing) Eddington-Finkelstein coordinates. The metric data on W are chosen to coincide with those of the Schwarzschild metric at that radius ($\beta = 0, V = 1 - 2M/r$). The coupled evolution of the Einstein-matter system produces dynamical spacetimes in the interior of W. The exterior region, initially described by the static black hole solution, will remain described consistently as such, provided that matter never reaches W. The relativistic hydrodynamic equations for a perfect fluid are formulated as a first-order flux-conservative hyperbolic system. The fluid is described completely by the rest-frame density ρ, the radial velocity u^r and the specific internal energy ε. The equation of state is $p = (\gamma - 1)\rho\varepsilon$, with $\gamma = 5/3$. The choice of fluid data on τ_0 fixes the metric functions β and V on that hypersur-

face. In turn those characterise the nature of the spacetime (e.g., the presence and size of a black hole). For vacuum data (no fluid), an apparent horizon, defined here as the spacelike two-sphere at which $V(\tau, r)=0$, will be present on the initial slice at $r = 2M$. With non-zero fluid mass, the initial location of the apparent horizon will shift towards smaller radii. In our framework, the presence of an apparent horizon is essential, as we rely on the concept of *excision* (See discussion in [14]), as applied to the characteristic initial value problem [15,16] for prescribing boundary conditions at the inner edge of the domain. Since the apparent horizon must be at least at $r = 0$, there is an upper bound to the amount of matter that can be prescribed to the interior of W. Further details of the implementation are given in [11]. See [13] for recent reviews on techniques.

Whereas the previous considerations provide us with a fairly faithful model of an accreting black hole spacetime, in order to identify the features of gravitational wave emission we resort to more idealised modelling. We capture the essence of non-spherical gravitational perturbations by solving the evolution equation for a minimally coupled mass-less scalar field $\Box \phi = (-g)^{-1/2}((-g)^{1/2}g^{\mu\nu}\phi_{,\mu})_{,\nu} = 0$. The spacetime background on which this equation is solved is the accreting black hole spacetime provided by the Einstein-matter evolution system described above. We assume vanishing stress-energy density for the scalar field. Physically, this setup closely models the dynamics of genuine spacetime perturbations, and any differences are primarily numerical in nature. Characteristic initial data for the scalar field equation consist of a single function $\phi_0(r)$ prescribed on the initial ingoing lightcone τ_0. Such data simulate the initial *shearing* of the in-going light-cone away from a pure spherically symmetric convergence. Non-trivial deviations from sphericity would be induced e.g., in the early phases of black hole formation due to asymmetries in the collapse process. We make the simplifying assumption that perturbations are not reinforced by any further inhomogeneities during the accretion process, i.e., we treat a decoupled and homogeneous problem for the wave equation. The linearity of the scalar field and the spherically symmetric background allow the expansion of ϕ into regular spherical harmonics $Y_{lm}(\theta, \phi)$ and lead to a decoupled set of evolution equations for each angular mode $g = r\phi_l(\tau, r)$:

$2g_{,\tau r} + (Vg_{,r}/r)_{,r} = (V/r)_{,r}g/r + l(l+1)e^{2\beta}g/r^2$. The integration procedure for this equation follows closely the techniques used in [17–19]. The algorithms are only slightly modified by the presence of a horizon, inside which outgoing characteristics converge. The radial grid used in our simulations extends from $r_{\min} = 0.6$ to $r_{\max} = 50$, with a resolution $\Delta r = (r_{\max} - r_{\min})/1800$. The radial grid for the scalar field evolution coincides with the spacetime grid for $r < r_{\max}$ and extends three times as much in the exterior, static region. This latter step allows us to effectively ignore the tricky question of what scalar field data to prescribe on the worldtube so as to model the unimpeded transmission of the wave into the static region.

We turn now our attention to the physical description of the accreting black hole spacetimes. The ratio $\lambda = M_{\rm i}/M_{\rm f}$ of the initial to final black hole mass is a first key parameter. For a minimally complete parameter space, this number must be accompanied by the average value of the accretion rate $\mu = <\dot{M}>$, which for fixed λ reflects the duration of the accretion event. We henceforth scale all distances and times (and derived quantities) by the mass of the final black hole which is always assumed to be unity ($M_{\rm f} = 1$). The collapse of a star to form a black hole can be considered as the limiting case in which $\lambda \to 0$. In the opposite limit ($\lambda \to 1$) we deal with infinitesimal changes to the black hole mass. Given the conventions above, the control of type of accretion event is entirely through the choice of the fluid data on the initial time surface. It is intuitively obvious that only accretion events on mass and time scales comparable to the size of the black hole horizon will have an appreciable effect on the QNM emission. We select here a family of fluid data that appears to be a fairly generic representative of fast and significant accretion of matter.

We choose an initial density profile that is radially constant up to a radius r_c and then decaying exponentially ($\rho_0(r) = \rho_c$ for $r < r_c$ and $\rho_0(r) = \rho_c e^{-\kappa(r-r_c)^2}$ for $r > r_c$, with $\kappa = 0.05$). The velocity and internal energy profiles are simple monotonically decreasing power laws ($u^r \sim r^{-0.5}, \varepsilon \sim r^{-1}$). The initial density distribution exerts the strongest influence on the evolution of the horizon, we hence keep the other fluid variables fixed to the above choices and vary the density profile via the parameters ρ_c and r_c. We turn next to the

5

initial data for the scalar field. Physically, the form (amplitude etc.) of the perturbation field at the initial time depends heavily on the spacetime history *prior* to the event simulated here. We make the assumption that such perturbations have a characteristic wavelength comparable to the size of the horizon at the initial time τ_0. We hence use $\phi_0(r) = \phi_p$ for $r < r_p$ (peak) and $\phi_0(r) = \phi_p e^{-\kappa(r-r_p)^2}$ for $r > r_p$. The amplitude ϕ_p is arbitrary. Exploration of the parameter space (r_p, κ) for the initial data suggests that differences in the profiles affect mostly the early phase of the signal (i.e., the prompt emission). In the results presented below we use $r_p = 1.06 M_{\mathrm{i}}$ and $\kappa = 2$.

Figure 1 displays a spacetime diagram of a representative accretion event. The diagram focuses on the innermost region of the computational domain, to help the identification of many of the key elements of the simulation. We see the evolution of the apparent horizon as a thick solid line. Representative streamlines (integrals of the velocity vector field) of accreting matter are shown as thin solid lines. The dotted lines foliating the spacetime diagram in Fig.1 form a central concept of the further analysis. They are the *zero phase surfaces* of the perturbation field ϕ_l. At a remote observer site those surfaces determine the zero crossings of the signal. The modulation of the period of the signal during the depicted accretion process is evident already from the figure, as can be seen from the variable intercept intervals, which grow longer at later times. In fact, the accretion is modulating both the decay rate and the oscillation frequency, as shown in the typical signal profile shown in Fig.3 Nevertheless, in the sequel we focus primarily on the QNM instantaneous *frequency*, which clearly is the most relevant aspect of the signal (a recent discussion of its relevance for GRW detection was given recently in [20]). Instantaneous values for the signal frequency (ISF) and its time derivative are obtained from the zero crossings of the field measured by an observer located at a fixed radius (here $r = 30$).

In Figure 2 we show the main features of the ISF evolution in the form of $\dot{f}(f)$ trajectories for different angular harmonic modes ($l = 2, 3, 4$) and different accretion rates. We see that all curves share the same broad characteristics. Initially, there is a rapid sweep into negative values of $\dot{f}$. This reflects the fast shedding of higher frequency (and higher damping

rate) overtones from the early emission, which results in a lower frequency signal. The evolution reaches a peak negative rate and then turns around and asymptotes to the vacuum oscillation frequency ($\dot{f}$=0). Different l modes are seen to reach different negative rates and seem to scale with the l value. This is a simple effect, due to the change of scale of the frequency of the underlying signal. We hence explore the effects of varying accretion rate by fixing $l = 3$. We present results for $r_c = (10, 15, 20)$ and peak densities $\rho_c \times 10^5 = (0.69, 0.2752, 0.1351)$, represented by empty diamonds, circles and crosses, respectively. All three choices correspond to $\lambda = 0.375$, i.e., a fixed ratio of initial to final black hole mass. The choice of r_c effectively controls the duration of the accretion event, albeit in a manner determined only *a posteriori*. It is seen that larger r_c values, that is, an initial distribution of the accreting mass within a larger volume, lead to larger variations of the frequency. The intuitive explanation of this effect uses loosely notions from vacuum black hole perturbation theory. A tenuous matter configuration implies a delayed growth for the black hole horizon. In turn this means the QNM frequency samples various "horizon sizes". A fast accretion, in turn, implies that most of the ringing is produced around a black hole that has already almost reached its final mass, hence the QNM frequency is mostly around that final value. The horizontal evolution of the QNM frequency during the emission is then seen to reflect on the amount of horizon growth during this era, whereas the elapsed time establishes the accretion rate. We'll see that for sufficiently slow accretion rates this statement can be made very precise by using a simple dimensional argument, but in the general case more detailed analysis would be required to extract the precise correlation. We note here that Figure 2 illustrates in passing two tests of the numerical procedure: i) A consistency test, represented by the vertical line at $f = 0.0769$. This is the value for the QNM frequency of a vacuum black hole (scalar $l = 2$ mode), as estimated by perturbation theory (WKB approaches) [21,2]. ii) An accuracy test, represented by the solid line overlaying the $l = 4$ sequence, obtained with twice the resolution in all parts of the algorithm.

In Figure 3 we show the late time behaviour of the negative branch in the $\dot{f}(f)$ diagram, for a simulation with $l = 3$ and $r_c = 15$ (this behaviour is also generic to the family explored

here). The solid line depicts the evolution of the mass accretion rate $\partial log(M)/\partial\tau$ versus observer time τ. We identify as mass M, the mass obtained from the radius of the apparent horizon $M = r_H/2$, whose location can be read off by identifying the location of the zero-crossing of the metric variable g_{00}. At late times the accretion flow slows to a trickle, and obeys a power law slope (in this case the slope equals -4.5). We find that the ISF curve itself follows a power law of the same slope at late times. For a more thorough comparison, we may overlay the two data sets after adopting a horizontal (time) offset for $\dot{M}(\tau)$ with respect to $\dot{f}(\tau)$. In the case shown this offset is $\tau_O = 71$. Perhaps not surprisingly, the best fit is produced by a value roughly corresponding to the travel time of a null geodesic from the strong field region around $r = 3$ to the observer location at $r = 30$. The good agreement of the slopes shows that the specific dynamics of the black hole growth in late times imprints itself rather directly on the ISF and is hence communicated via gravitational waves to the exterior domain. The QNM frequencies for a vacuum black hole of mass M obeys a scaling relation $\omega = \sigma/M$, where σ depends only on the overall shape of the potential black hole potential. For sufficiently small $\dot{\sigma}$ we obtain that the logarithmic derivative of the frequency equals the negative logarithmic accretion rate ($\partial log(f)/\partial\tau = -\partial log(M)/\partial\tau$). We have seen in Figure 3 that indeed this behaviour is dominant in late times, suggesting indeed that $\dot{\sigma}$ is small in this scenario.

It may be useful to try to establish closer connections with vacuum black hole perturbation theory. By introducing a coordinate $x(r)$ (generalising the *tortoise* coordinate [1]) governed by $dx/dr = r/V$, the wave equation for a scalar field on a growing black hole background reads $2g_{,x\tau} + Cg_{,xx} + Dg_{,r} + Pg = 0$ where $C = 1 + 2dx/d\tau$, $D = -V_{,\tau}/r$ and $P = -V/r[(V/r)_{,r}/r + l(l+1)e^{2\beta}/r^2]$. This equation generalises analogous expressions for static black holes. The function $P(\tau, r)$ may be thought of as an "instantaneous" effective potential. The dashed line in Figure 1 illustrates the outward motion of the maximum of this function. The trajectory $r_P(\tau)$ follows quite closely the horizon motion, and interestingly, the ratio $r_P(\tau)/r_H(\tau)$ is found to be almost constant as a function of time, irrespective of the accretion rate (hence equal to the value of that ratio for a *static* black hole). This is

somewhat surprising, as it implies that $\dot{\sigma}$ is almost zero. While this is consistent with the late time agreement of Fig.3, we see that at early times the frequency evolution is visibly different from the mass evolution. We conclude then that at early times (and rapid accretion), the dynamics is more subtle than the one deduced from dimensional arguments, but potentially explainable through the additional terms in the generalised wave equation introduced above.

REFERENCES

[1] S. Chandrasekhar, *The Mathematical Theory of Black Holes*, Oxford University Press (1983).

[2] K.D. Kokkotas and B. Schmidt, Living Reviews in Relativity, 1999-2 (1999)

[3] N. Andersson, Phys. Rev. D, **55**, 468 (1997)

[4] J. Oppenheimer and H. Snyder, Phys. Rev., **56**, 455 (1939)

[5] M. May and R. White, Phys. Rev., **141**, 1232 (1966)

[6] C. T. Cunningham, R.H. Price and V. Moncrief, Astrophys. J., **224**, 643 (1978)

[7] E. Seidel, Phys. Rev. D, **44**, 950 (1991)

[8] R. F. Stark and T. Piran, Phys. Rev. Lett. , **55**, 891 (1985)

[9] R. Popham, S. Woosley and C. Frier, Astrophys. J., **518**, 356 (199)

[10] P. T. Leung, Y. T. Liu, W.-M. Suen, C. Y. Tam and K. Young, Phys. Rev. Lett. , **78**, 2894 (1997)

[11] P. Papadopoulos and J. A. Font, Phys. Rev. D, **61**, 024015 (2000)

[12] L.A. Tamburino, and J. Winicour, Phys. Rev., 150, 4, 1039 (1966)

[13] J. A. Font, Living Reviews in Relativity, 2000-2 (2000)

[14] G.B. Cook et al., Phys. Rev. Lett. , **80**, 2512 (1998)

[15] R. Gómez, L. Lehner, R. Marsa and J. Winicour, Phys. Rev. D, **57**, 4778 (1998)

[16] R. Gómez, R. Marsa and J. Winicour, Phys. Rev. D, **56**, 6310 (1997)

[17] R. Gómez, R. Isaacson and J. Winicour, J. Comput. Phys., **98**, 11 (1992)

[18] R. Gómez, P. Papadopoulos and J. Winicour, J. Math. Phys., **35**, 4184 (1994)

[19] R. Gómez, *et al.*, Phys. Rev. Lett. , **80**, 1000 (1998)

[20] M.H.P.M. van Putten and A. Sarkar, Phys. Rev. D, **62**, 041502 (2000)

[21] S. Iyer, Phys. Rev. D, **35**, 3632 (1987)

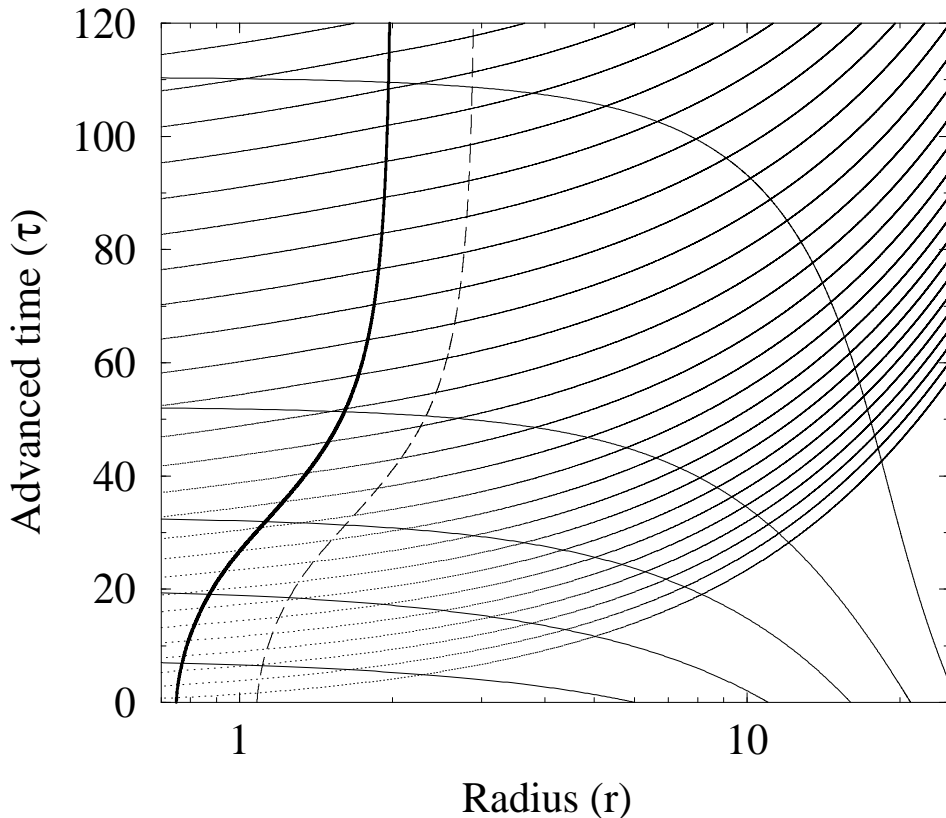[22] K. Kokkotas and B. Schutz, Phys. Rev. D, **37**, 3378 (1988)

FIG. 1.   Scalar field dynamics on an accreting black hole spacetime. The thick solid line is the trajectory $r_H(\tau)$ of the apparent horizon, starting from the initial value $r = 0.75$ and growing to the final value $r = 2$. The infall of fluid matter is illustrated by representative streamlines, shown as thin solid lines. The lines start at initial radii $r_i = 6 + (i-1)5$, with $i = 1, \ldots, 5$. The dotted lines foliating the diagram are the zero phase surfaces of the perturbation field ϕ_l. For any given field multipole, the diagram represents the appearance of the gravitational wave generation and propagation for a fixed set of angular directions (θ, ϕ). The zero phase surfaces tend asymptotically to outgoing light cones (the use of a logarithmic plot obscures this somewhat in the diagram), but are clearly spacelike near the horizon. It is readily seen that an observer located at a constant radius will intercept zero phase signals of initially shorter periods which progressively increase and asymptote to the QNM period of the final black hole. Tracing back the zero phase surface to the horizon region illustrates how the size of the horizon is associated with the temporal separation of successive levels.
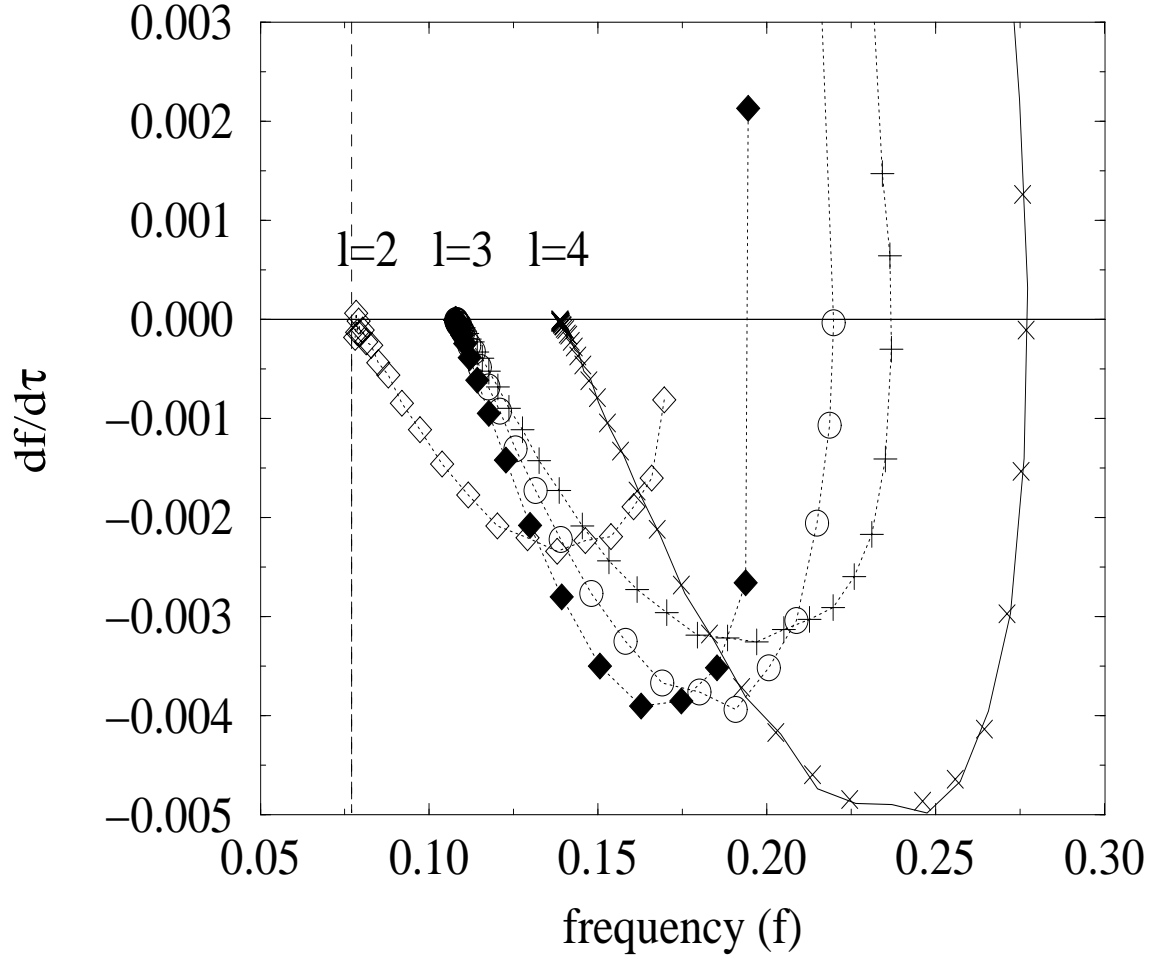
FIG. 2. Frequency time derivative versus frequency. The symbols (crosses, circles etc.) denote instances at which a zero crossing event enables the computation of an instantaneous frequency and its time derivative. The fitted lines aid the reading of the trajectories. Common to all evolutions is the rapid sweep into negative $\dot{f}$ in the early phase of the signal. The evolution reaches its peak (negative) $\dot{f}$ and as the accretion ceases asymptotes to the vacuum oscillation frequency ($\dot{f}$=0). Different l modes provide qualitatively similar probes of the frequency dynamics, but with an overall magnitude difference. The vertical dashed line at $f = 0.0769$ denotes the frequency of a scalar ($l = 2$) *vacuum* black oscillation (of the same final mass), as estimated by a higher order WKB approximation. The solid line overlaying the $l = 4$ sequence is obtained with double resolution in all parts of the algorithm and indicates that the resolution used is sufficient.
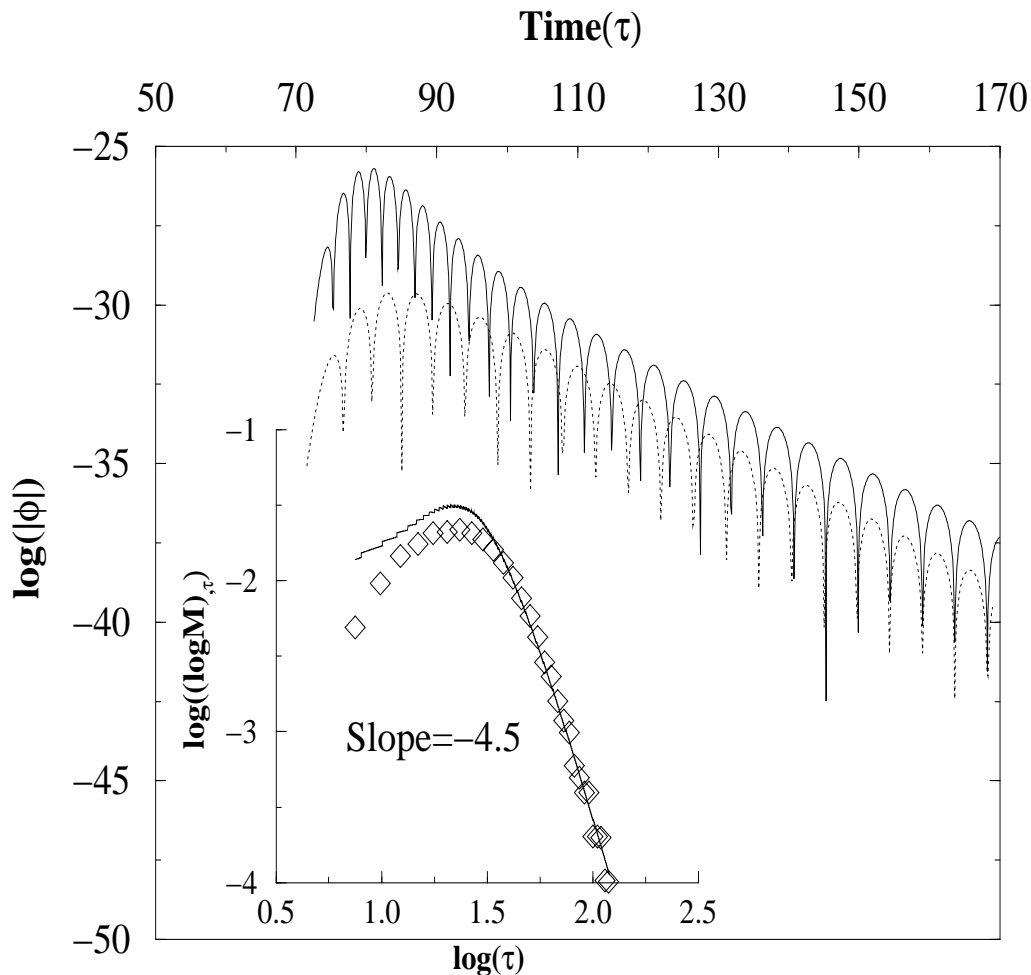
FIG. 3. Typical modulated waveforms and correlations between frequency and accretion rates. The logarithm of the signal is shown as a function of time for an $l = 3$ and $r_c = 15$ simulation (solid line). The dotted line indicates the ringdown of a *vacuum* black hole with $M = 1$. The decay rate modulation is particularly evident here. We have not analysed this effect quantitatively. The insert shows the late time behaviour of the signal frequency in correlation with the accretion rate, as a function of time (same simulation) The solid line depicts the evolution of the accretion rate $dlog(M)/d\tau$ versus observer time τ. That quantity is derived from the location of the horizon and is governed directly by the amount of inflowing fluid. Overlayed on the mass accretion rate is the logarithmic time derivative of the signal frequency. At late times the accretion flow leads to a power law slope (in this case the slope equals -4.5) and we find that the ISF curve itself follows a power law of the same slope.